This article has been accepted for publication in a future issue of this journal, but has not been fully edited. Content may change prior to final publication. Citation information: DOI 10.1109/TPWRD.2019.2938020, IEEE Transactions on Power Delivery

Estimating Power Transformer High frequency Model Parameters using Frequency Response Analysis

A. Abu-Siada, M. I. Mosaad, Do Won Kim and Mohamed F. El-Naggar

***Abstract*— Frequency response analysis (FRA) has become a widely accepted technique by worldwide utilities to detect winding and core deformations within power transformers. The main drawback of this technique is its reliance on the personnel level of expertise more than standard or automated codes. To establish reliable FRA interpretation codes, accurate high frequency transformer model that can emulate the frequency characteristics of real transformers in a wide frequency range is essential. The model can be used to investigate the impact of various winding and core deformations on the transformer FRA signature. The transformer equivalent high frequency electric circuit parameters can be calculated based on design data, which are rarely available, especially for old transformers. As such, this paper presents an artificial intelligence technique to estimate these parameters from the transformer FRA signature. The robustness of the proposed technique is assessed through its application on three, 3-phase power transformers of different ratings, sizes, and winding structures to estimate their high frequency electric circuit parameters during normal and fault conditions. Results show that the proposed technique can estimate equivalent circuit parameters with high accuracy and helps interpret the FRA signature based on the numerical changes of these parameters. The main advantage of this approach is the physical meaning of the model parameters facilitates reliable identification of various faults and hence aids in establishing reliable interpretation codes for transformer FRA signatures.**

***Index Terms* – High frequency transformer modeling, Parameters estimation, Frequency response analysis, Genetic algorithm, Particle swarm optimization.**

I. INTRODUCTION

AS power transformer is a critical asset in electricity grids, reliable fault diagnostic techniques should be adopted to avoid any catastrophic consequences including outages, fire, serious injuries, and revenue loss [1, 2]. Among these techniques, frequency response analysis (FRA) has been widely used to diagnose the transformer mechanical integrity [3-6]. FRA technique has been also utilised to detect transformer bushing failure and insulation system degradation [7, 8]. The idea of this technique was originated from the fact that a power transformer can be modeled as an electric circuit of capacitive, resistive and inductive parameters that represent various transformer components including core, winding and insulation system. Any mechanical deformation or insulation system degradation lead to a change in these parameters which can be detected through the comparison of the transformer frequency characteristic with a reference signature or by comparing the FRA responses of the three individual phases in each side. The main drawback of the FRA technique is its reliance on the personnel level of expertise more than standard or automated codes. This may result in false or inconsistent interpretation for the measured FRA signatures. To overcome this limitation research efforts have been conducted and published in the literature in order to automate and standardize the FRA interpretation process. For instance, [9-11] present a new polar plot FRA signature that can be compared with the transformer fingerprint using digital signal processing technique to identify and quantify various faults within the transformer. However, this technique is still immature and needs to be validated through practical implementation across a wide range of operating power transformers. It is impractical to stage various fault types with different levels on operating transformers to examine their effects on the FRA signature. Hence, to establish a standard interpretation code for FRA signatures, reliable transformer high frequency model is essential. While power frequency transformer model parameters can be identified through conducting some experimental measurements such as open and short circuit tests [12, 13], high frequency transformer model parameters are calculated based on precise geometric dimensions of the transformer, which may not be available due to manufacture confidentiality. Some attempts to estimate the parameters of transformer equivalent circuit at the power frequency (50 or 60 Hz) based on non-experimental data can be found in the literatures [14-21]. However, estimating the parameters of a transformer high frequency model for accurate FRA studies was not given much attention. Furthermore, the practical application of such model parameters to identify and quantify various transformer faults has not been explored yet. The transformer FRA signature could be in the form of impedance, admittance, or transfer function (TF) in a wide frequency range.

Various combinations of transformer terminals connection along with recommended TF for frequency response studies can be found in [22]. The FRA signature comprises resonance frequencies representing zeros and poles of the winding impedance, admittance or TF that can be employed to estimate the transformer equivalent electric circuit parameters. Few studies on estimating the high frequency transformer parameters can be found in the literature. For instance, in [23], FRA is employed to only measure the transformer complex short circuit impedance. Identification of transformer core parameters including magnetic permeability and electrical conductivity using FRA is presented in [24]. Transformer parameters are estimated in [25] using least nonlinear square and maximum likelihood methods. However, circuit parameters could be only estimated in the low frequency range. Furthermore, the proposed method comprises complex calculations. Vector fitting technique can be employed to estimate transformer winding parameters based on the resonant frequencies of the FRA signature [26]. However, models developed based on this technique may not exhibit consistent high accuracy for all properties of the physical system. As reported in [27], a model developed based on winding impedance matrix may result in unsatisfactory performance for calculations based on admittance matrix and vice versa. To overcome this issue, a modal vector fitting technique utilizing eigenvalues rather than matrix elements has been proposed in [27].

This article has been accepted for publication in a future issue of this journal, but has not been fully edited. Content may change prior to final publication. Citation information: DOI 10.1109/TPWRD.2019.2938020, IEEE Transactions on Power Delivery

Precise estimation of the electrical parameters of a comprehensive high frequency transformer model will facilitate a better understanding to the impact of various mechanical winding and core deformations on the FRA signature. This paper presents an effective application of artificial intelligence (AI) techniques to estimate the electrical parameters of a comprehensive high frequency model from the transformer FRA signature. The proposed technique can be utilized for power transformer fault identification and quantification in which the numerical values of the equivalent circuit parameters of the healthy transformer can be stored as a transformer fingerprint for future comparison. Unlike the current FRA industry practice which relies on graphical comparison that may lead to inconsistent interpretation for the same FRA signature, the physical meaning of the electrical model parameters results in more consistent and reliable analysis. Two AI techniques; genetic algorithm (GA) and particle swarm optimization (PSO) are employed to estimate the equivalent circuit parameters of two, 3-phase transformers of different sizes, windings structures and ratings (10 kVA and 40 MVA) during normal and fault conditions. The practical implementation of the proposed technique is also presented through its application on a practical FRA measured signature of a faulty transformer.

II. TRANSFORMER MODELLING

High frequency transformer model can be represented by equivalent ladder or lumped electric circuit that represents a single disk or turn. The transformer overall model can be simulated by connecting multiple number of this circuit in cascade based on the number of turns/disks of the transformer. Also, the transformer can be simulated as a multi-conductor transmission line using state space representation [28]. The high frequency transformer equivalent circuit of one disk/turn comprises resistive, inductive, and capacitive parameters as shown in Fig. 1.

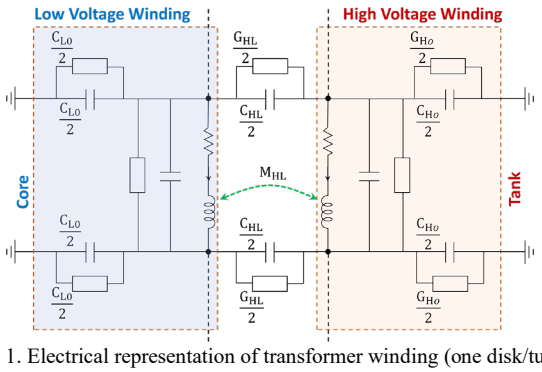

Fig. 1. Electrical representation of transformer winding (one disk/turn).

In the transformer high frequency equivalent circuit shown in Fig. 1, the high voltage (HV) and low voltage (LV) windings are represented by series resistance (R) and inductance (L) shunted by capacitance (C_{sh}) and conductance (G_{sh}). The insulation between the two windings is modeled by capacitance (C_{HL}) shunted by a dielectric conductance (G_{HL}) while (M_{HL}) represents the mutual inductance between the two windings. The dielectric insulation between the LV winding and the earthed core and the insulation between the HV winding and the earthed tank are simulated by a capacitance (C_0) and dielectric conductance (G_0). For FRA practical measurements, co-axial cables of 50 Ω are used to connect the frequency response analyzer to the input and output terminals of the transformer windings. This has to be considered to drive the transfer function of each transformer winding. Table I shows the relevance of electric model parameters and various mechanical faults that a transformer may exhibit during its operational life.

Table I
Transformer model parameters and associated mechanical faults

Parameter	Type of Fault
Self/mutual Inductance	Winding / Core deformation, shorted turns and disk space variation.
Shunt Capacitance	Disk space variation, winding buckling and loss of clamping pressure.
Series Capacitance	Insulation degradation and disk movement.
Resistance	Shorted turns.

III. ARTIFICIAL INTELLIGENCE ALGORITHMS

AI algorithms have been successfully used for solving complex nonlinear equations and optimization problems [29]. GA and PSO have been used to estimate the transformer equivalent circuit parameters at power frequency from transformer nameplate data [15] as well as estimating the induction motor and PV parameters [30, 31]. The common concept of both techniques is developed based on iterative approach using parallel processing of a guided random search for optimum solution [32]. The evolutionary biological mechanism is the main inspiration of developing the GA technique. On the other hand, PSO technique was inspired through the attitude of some creatures such as fish schools, bird flocks and bee swarm [33]. The performance of optimization techniques depends on the selection of a proper fitness or objective function. In this paper, the fitness function is developed to estimate the optimum set of the circuit parameters shown in Fig. 1 based on the transformer winding transfer function.

To track peaks and valleys and curves connecting them accurately, the proposed objective function J is divided into two terms; J_1 and J_2 as below.

$$J_1 = \sum_{i=1}^{k}\left(\frac{(|\mathrm{TF}|i)_{measured} - (|\mathrm{TF}|i_{estimated}}{(|\mathrm{TF}|i)_{measured}}\right)^2 \quad (1)$$

$$J_2 = \sum_{i=1}^{n}\left(\frac{(|\mathrm{TF}|ir)_{measured} - (|\mathrm{TF}|ir)_{estimated}}{(|\mathrm{TF}|i)_{measured}}\right)^2 \quad (2)$$

where $(|\mathrm{TF}|_i)_{\mathrm{measured}}$ and $(|\mathrm{TF}|_i)_{\mathrm{estimated}}$ are respectively the magnitude of the measured and estimated FRA signatures at any frequency point i, and k is the total number of frequency points. $(|\mathrm{TF}|_{ir})_{measured}$ and $(|\mathrm{TF}|_{ir})_{estimated}$ are the magnitudes of the measured and estimated FRA signature at any resonant frequency point ir; respectively and n is the number of resonance frequencies.

Then the proposed objective function (J) comprising (1) and (2) can be written as:

$$J = J_1 + J_2 \quad (3)$$

The two AI techniques used to minimise J are elaborated below.

A. Genetic algorithm

In this algorithm, the objective function evaluates the estimated parameters (optimized population) in order to maintain the chromosomes (electrical circuit parameters) of

This article has been accepted for publication in a future issue of this journal, but has not been fully edited. Content may change prior to final publication. Citation information: DOI 10.1109/TPWRD.2019.2938020, IEEE Transactions on Power Delivery

high fitness in the new generation by ranking population individuals. The methodology of GA is shown by the blue color in the flow chart of Fig. 2 and is briefly elaborated below [32].

- *Initialization*: a random population for the 8 electrical parameters (R_s, L_s, C_{sh}, G_{sh}, C_0, G_0, C_{HL}, and G_{HL}) is created.
- *Evaluation*: based on the parameters defined in the previous step and the equivalent circuit of Fig. 1, the estimated TF is calculated and is compared with the actual FRA measured signature to evaluate the objective function in (3).
- *Updating*: a new population is created by applying selection and reproduction operators (elitism, crossover and mutation) and the best-fitted individuals are copied to the newly created population.
- *Termination*: the above updating process is repeated till a global minimum value for the objective function or a maximum number of iterations is achieved.

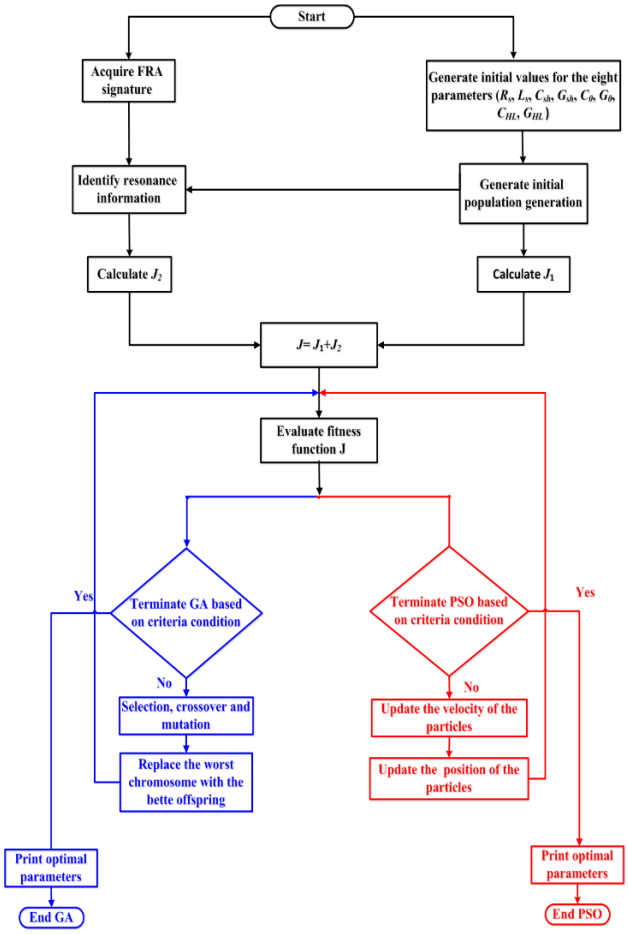

Fig. 2. Flow chart of GA and PSO optimization techniques.

B. Particle swarm optimization

The population in the PSO for the estimation process includes eight parameters (R_s, L_s, C_{sh}, G_{sh}, C_0, G_0, C_{HL}, G_{HL}). Unlike GA which modifies population from generation to generation, PSO keeps the same population and updates the position of the population particles which flies through a search space with a velocity that is updated by movement inertia, self-cognition and social interaction [33]. During each generation individual particles are accelerated to reduce its distance from the global optimum position. The particle velocity (V) and position (X) are updated using the equations below:

$$V_m^{k+1} = \omega V_m^k + c_1 r_{1_m}^k (P_m^k - X_m^k) + c_2 r_{2_m}^k (P_{pb}^k - X_m^k) \quad (4)$$

$$X_m^{k+1} = X_m^k + V_m^{k+1} \quad (5)$$

where k is the iteration number, c_1 and c_2 are cognitive and social acceleration parameters, r_1 and r_2 are random numbers uniformly distributed between 0 and 1, P_i is the best-known position of a particle m, P_{pb} is the best-known position within the population and w is the particle inertia.

Fig. 2 shows the flow chart of PSO methodology (in red color) which is quite similar to the GA described above except for updating the parameters through updating particles velocity and position using (4) and (5), respectively.

IV. SIMULATION AND PRACTICAL CASE STUDIES

As discussed in the introduction section, the electrical parameters of the high frequency power transformer model can be calculated using detailed physical dimensions of the transformer using set of empirical equations or through 3D finite element analysis (FEA) simulation [2]. FEA is a computer-based method that is widely accepted as a reliable tool to simulate the real operation of power transformers. In this paper, FEA is used to build 3D models for two, 3-phase transformers of different ratings (10 kVA and 40 MVA), and windings structures as shown in Fig. 3. The 10-kVA transformer windings are of rectangular structure in which the LV winding is a continuous layer of 140 turns and the HV winding comprises 6 disks of 1134 turns each. On the other hand, the windings of the 40-MVA transformer are of circular configuration with a continuous LV winding of 200 turns and 10-disk HV winding type of 120 turns each. The physical dimensions of the two transformers are as shown in Fig. 4 [2, 9].

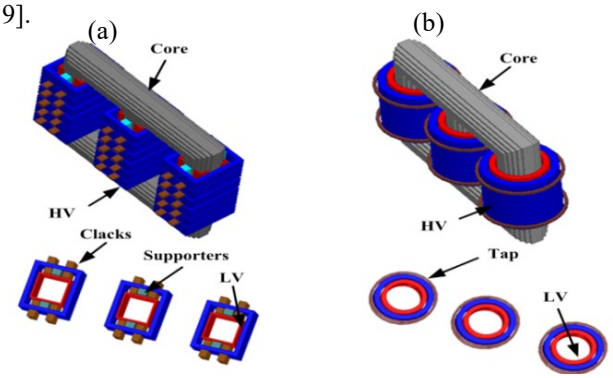

Fig. 3. 3D transformer models: (a) 10 kVA, (b) 40 MVA.

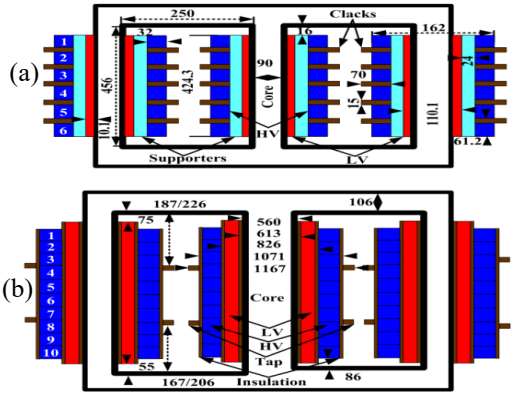

Fig.4. Transformer physical dimensions (mm) (a) 10-kVA, (b) 40-MVA.

This article has been accepted for publication in a future issue of this journal, but has not been fully edited. Content may change prior to final publication. Citation information: DOI 10.1109/TPWRD.2019.2938020, IEEE Transactions on Power Delivery

The 3D finite element transformer model is solved in magnetostatic and electrostatic solvers using Maxwell equations to extract the inductive, capacitive components while eddy current is used to calculate resistive components [34]. Inductance calculation is conducted using the magnetic energy stored in a particular volume of the conductor while capacitance is calculated based on the electrostatic energy and the potential difference between two adjacent conductors. Equations for calculating these parameters along with the parameters of the equivalent circuit of the two investigated transformers calculated by FEA are respectively listed in Tables A-I and A-II in the Appendix. Multiple circuits of the model shown in Fig. 1 are connected in cascade according to the number of disks of each transformer and is simulated using MATLAB/Simulink software. To simplify the model, the conductance of the insulation system is neglected and the mutual inductances are lumped into the series inductances. The FRA signatures of the LV and HV windings of each transformer based on the circuit parameters calculated by the FEA is obtained by injecting a sinusoidal voltage of low amplitude and variable frequency (up to 1 MHz) to one winding terminal and capturing the response at the other terminal. In this paper, the FRA signature is presented in the form of winding transfer function in dB ($|TF| = \frac{V_{output}}{V_{input}}$).

The TF of each winding can be also obtained using the state space representation of the transformer equivalent circuit. The differential equations of the state variables (voltage across each capacitance and current through inductance) can be obtained by applying Kirchhoff's laws at various nodes of the equivalent electric circuit as shown in Fig. A-1 and equations (A.1) and (A.2) in the Appendix.

The obtained FRA signatures are then used to estimate the electrical parameters of the investigated transformers using the two proposed AI techniques. The estimated parameters are compared with the electrical parameters calculated using FEA. The accuracy of the proposed estimation techniques is assessed based on the degree of consistency between the FRA signatures obtained using the circuit parameters calculated by the FEA and the parameters estimated using the proposed AI-techniques. To increase the degree of consistency between the calculated and estimated FRA signatures, two sub-objective functions (J_1 and J_2) are proposed as presented in the section III. J_1 is introduced to compare the two signatures over the entire frequency range, while J_2 is proposed to enhance the consistency of the two signatures at the resonance frequencies. In this context, a Matlab code is developed to calculate the magnitude of the estimated TF at each frequency point and compare it to the TF obtained from FEA to form J_1. Another code is developed to extract all resonance frequencies with the corresponding TF magnitudes to form J_2. Proposed AI techniques are used to minimize the main objective function J (sum of J_1 and J_2) to increase the degree of consistency between the calculated and estimated FRA signatures.

1. *Case study 1: 10-kVA transformer*

The eight transformer equivalent circuit parameters are estimated using GA and PSO techniques for both LV and HV windings as listed in Table II along with the values calculated using FEA. The percentage absolute error in each parameter (x) when estimated (using AI algorithms) and calculated (using FEA) is obtained as below:

$$Error\% = \left|\frac{x_{calculated} - x_{estimated}}{x_{calculated}}\right| x100\% \quad (6)$$

The convergence of the proposed objective function using GA and PSO for LV and HV windings is shown in Fig.5. The figure shows the rapid convergence of the two AI techniques as both start to converge at iteration number 20.

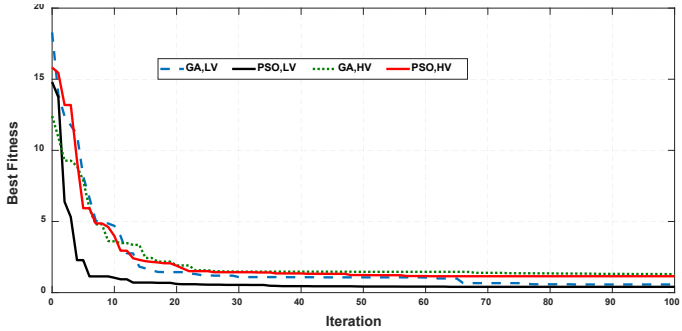

Fig.5. Convergence of the best fitness for LV and HV windings of the 10-kVA transformer.

The low percentage error shown in Table II reveals the ability of both AI techniques to estimate transformer equivalent circuit parameters from the FRA signature with an acceptable accuracy level. The estimated results are utilized to plot the FRA signature of the transformer equivalent circuit. Fig. 6 shows the FRA signatures of phase-A of the 10-kVA transformer (LV and HV) windings using calculated (FEA) and estimated (GA and PSO) circuit parameters.

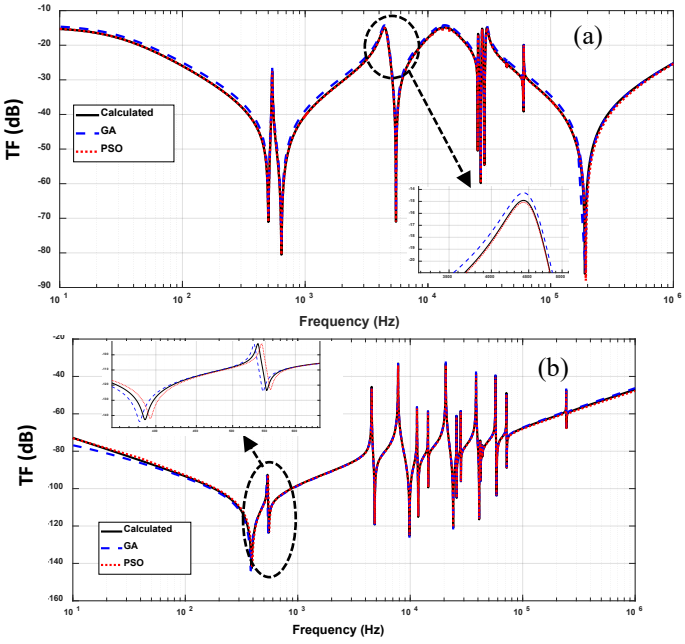

Fig. 6. Calculated and estimated FRA signatures of phase-A of the 10-kVA transformer (a) LV winding and (b) HV winding.

The FRA signature shown in Fig. 6 is characterized by multiple resonant points. In the low frequency range and due to the significant impact of the magnetic flux, the signature is dominated by the inductive components. In the high frequency range, capacitive components govern the signature while

This article has been accepted for publication in a future issue of this journal, but has not been fully edited. Content may change prior to final publication. Citation information: DOI 10.1109/TPWRD.2019.2938020, IEEE Transactions on Power Delivery

combined effect of both reactive components generates more resonant points in the mid frequency range. Results in Fig. 6 reveal high agreement between the FRA signatures plotted using estimated and calculated parameters. To assess the capability of the proposed estimation technique to detect changes in the equivalent electrical circuit parameters due to winding deformations, the values of C_{sh} and C_{HL} of the LV and HV windings are changed by 10% to simulate winding axial displacement [27]. The same two parameters are also changed by 20% to investigate the impact of various levels of axial displacement on the proposed estimation techniques. The estimated parameters of the LV and HV windings under these fault levels are listed in Tables III and IV; respectively. Phase-A HV and LV FRA signatures for each fault level using estimated and calculated parameters are shown in Figs. 7 and 8; respectively. These results reveal the ability of the proposed estimation technique to track the changes in the equivalent circuit parameters. This feature can be effectively used to identify and quantify various mechanical deformations within the transformer windings.

2. *Case study 2: 40-MVA transformer*

To assess the robustness of the proposed techniques to estimate the equivalent circuit parameters of power transformers of various ratings and winding structure, the GA and PSO proposed techniques are employed to estimate the electrical parameters of the 40-MVA transformer shown in Fig. 4(b). The estimated parameters of the LV and HV windings are listed in Table V.

Table II
Equivalent parameters of the 10-kVA transformer LV and HV healthy windings

Parameters	LV side					HV side				
	Actual	GA	Error %	PSO	Error %	Actual	GA	Error %	PSO	Error %
R_s [Ω]	0.5	0.45	10.00	0.56	12.00	1	0.94	6.00	1.05	5.00
L_s [μH]	20	21.21	6.05	22.31	11.55	40	39.2	2.00	40.1	0.25
C_{sh} [pF]	37.27	36.72	1.48	38.03	2.04	2.35	2.2	6.38	2.4	2.13
G_{sh} [μS]	260.89	256.77	1.58	259.32	0.60	6.45	6.11	5.27	6.52	1.09
C_o [pF]	718	723	0.70	721	0.42	20	21.3	6.50	20.8	4.00
G_o [μS]	5026	5029	0.06	5032	0.12	140	143	2.14	141.5	1.07
C_{HL} [pF]	50	48.51	2.98	51.33	2.66	50	48.8	2.40	51.4	2.80
G_{HL} [μS]	350	347.74	0.65	354.18	1.19	350	348.2	0.51	353.6	1.03

Table III
Equivalent parameters of the 10-kVA transformer LV winding with 10% and 20% change in C_{sh} and C_{HL}

Parameters	Actual	10 % change	GA	Error %	PSO	Error %	20% change	GA	Error %	PSO	Error %
R_s [Ω]	0.5	0.5	0.46	8.00	0.54	8.00	0.5	0.46	8.00	0.52	4.00
L_s [μH]	20	20	21.9	9.50	21.88	9.40	20	22	10.00	21.5	7.50
C_{sh} [pF]	37.27	33.5	35	4.48	34.8	3.88	29.8	31	4.03	30.8	3.36
G_{sh} [μS]	260.89	260.89	257	1.49	255.5	2.07	260.89	255	2.26	263	0.81
C_o [pF]	718	718	725	0.97	722.2	0.58	718	710	1.11	723.25	0.73
G_o [μS]	5026	5026	5002	0.48	5033	0.14	5026	5010	0.32	5035	0.18
C_{HL} [pF]	50	55	50.9	7.45	53	3.64	60	54.1	9.83	55.9	6.83
G_{HL} [μS]	350	350	345.8	1.20	353.7	1.06	350	347	0.86	352	0.57

Table IV
Equivalent parameters of the 10-kVA transformer HV winding with 10% and 20% change in C_{sh} and C_{HL}

Parameters	Actual	10 % change	GA	Error %	PSO	Error %	20 % change	GA	Error %	PSO	Error %
R_s [Ω]	1	1	1.1	10.00	1.15	15.00	1	0.92	8.00	1.05	5.00
L_s [μH]	40	40	37.5	6.25	42.2	5.50	40	38.5	3.75	40.9	2.25
C_{sh} [pF]	2.35	2.1	1.95	7.14	2.2	4.76	1.88	1.72	8.51	1.96	4.26
G_{sh} [μS]	6.45	6.45	5.8	10.08	7.2	11.63	6.45	5.75	10.85	6.7	3.88
C_o [pF]	20	20	18.2	9.00	21	5.00	20	18.3	8.50	20.85	4.25
G_o [μS]	140	140	132	5.71	144	2.86	140	131.5	6.07	144.8	3.43
C_{HL} [pF]	50	55	51	7.27	56.5	2.73	60	63.8	6.33	63	5.00
G_{HL} [μS]	350	350	346	1.14	352	0.57	350	346.5	1.00	351	0.29

Table V
Equivalent parameters of the 40-MVA transformer LV and HV healthy windings

Parameters	LV side					HV side				
	Actual	GA	Error %	PSO	Error %	Actual	GA	Error %	PSO	Error %
R_s [Ω]	0.25	0.23	8.00	0.22	12.00	1	0.92	8.00	0.95	5.00
L_s [μH]	10.5	12.12	15.43	11.98	14.10	10	9.82	1.80	10.15	1.50
C_{sh} [pF]	127.67	126.43	0.97	124.54	2.45	393.4	396.5	0.79	394.1	0.18
G_{sh} [μS]	63.835	61.44	3.75	62.03	2.83	196.7	200	1.68	198.5	0.92
C_o [pF]	115.53	116.43	0.78	117.72	1.90	61.19	60.92	0.44	61.85	1.08
G_o [μS]	57.765	55.32	4.23	58.91	1.98	30.59	29.89	2.29	31.2	1.99
C_{HL} [pF]	89.283	88.32	1.08	90.11	0.93	89.28	88.97	0.35	88.59	0.77
G_{HL} [μS]	44.65	42.8	4.14	45.8	2.58	44.65	41	8.17	46	3.02

This article has been accepted for publication in a future issue of this journal, but has not been fully edited. Content may change prior to final publication. Citation information: DOI 10.1109/TPWRD.2019.2938020, IEEE Transactions on Power Delivery

Table VI
Equivalent parameters of the 40-MVA transformer LV winding with 10% and 20% change in C_{sh} and C_{HL}

Parameters	Actual	10 % change	GA	Error %	PSO	Error %	20 % change	GA	Error %	PSO	Error %
R_s [Ω]	0.25	0.25	0.21	16.00	0.26	4.00	0.25	0.22	12.00	0.265	6.00
L_s [μH]	10.5	10.5	8.95	14.76	11.25	7.14	10.5	9.1	13.33	11.3	7.62
C_{sh} [pF]	127.67	115	99	13.91	123	6.96	102	97	4.90	110	7.84
G_{sh} [μS]	63.835	63.835	59	7.57	68	6.52	63.835	58.9	7.73	67	4.96
C_o [pF]	115.53	115.53	111	3.92	121	4.73	115.53	120	3.87	119	3.00
G_o [μS]	57.765	57.765	62	7.33	61	5.60	57.765	61	5.60	59	2.14
C_{HL} [pF]	89.283	98	92	6.12	103	5.10	107	104	2.80	111	3.74
G_{HL} [μS]	44.65	44.65	47.8	7.05	47.55	6.49	44.65	48	7.50	47.8	7.05

Table VII
Equivalent parameters of the 40-MVA transformer HV winding with 10% and 20% change in C_{sh} and C_{HL}

Parameters	Actual	10 % change	GA	Error %	PSO	Error %	20 % change	GA	Error %	PSO	Error %
R_s [Ω]	1	1	0.9	10.00	1.1	10.00	1	1.15	15.00	1.12	12.00
L_s [μH]	10	10	9.6	4.00	10.2	2.00	10	9.2	8.00	10.4	4.00
C_{sh} [pF]	393.4	355	340	4.23	348	1.97	315	308.3	2.13	321.6	2.10
G_{sh} [μS]	196.7	196.7	189	3.91	203	3.20	196.7	201.2	2.29	200.8	2.08
C_o [pF]	61.192	61.192	65	6.22	64.2	4.92	61.192	58.3	4.73	63.4	3.61
G_o [μS]	30.596	30.596	34	11.13	36	17.66	30.596	27.2	11.10	32.1	4.92
C_{HL} [pF]	89.283	98	92	6.12	92.4	5.71	107	111	3.73	110	2.80
G_{HL} [μS]	44.65	44.65	42	5.94	45	0.78	44.65	46.1	3.25	45.8	2.58

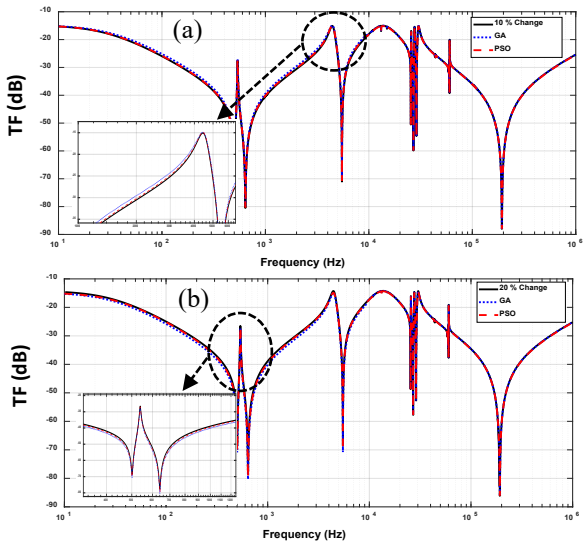

Fig.7. Calculated and estimated FRA for the 10-kVA transformer, LV winding using GA and PSO with change in C_{sh} and C_{HL} (a) 10%, (b) 20%.

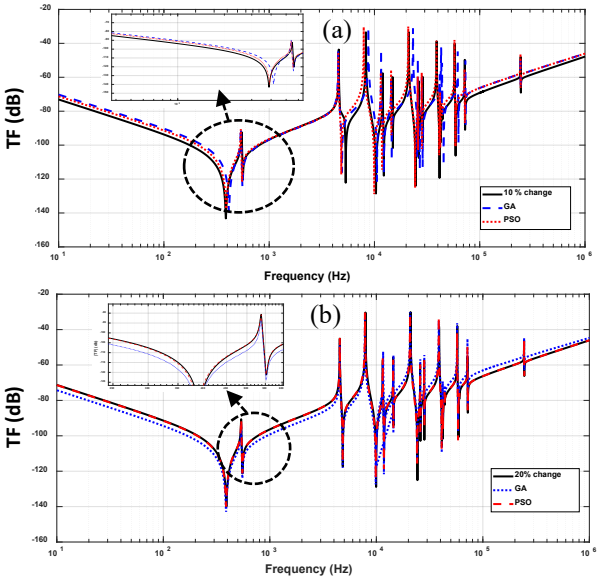

Fig.8. Calculated and estimated FRA for 10-kVA transformer, HV winding using GA and PSO with change in C_{sh} and C_{HL} (a) 10%, (b) 20%.

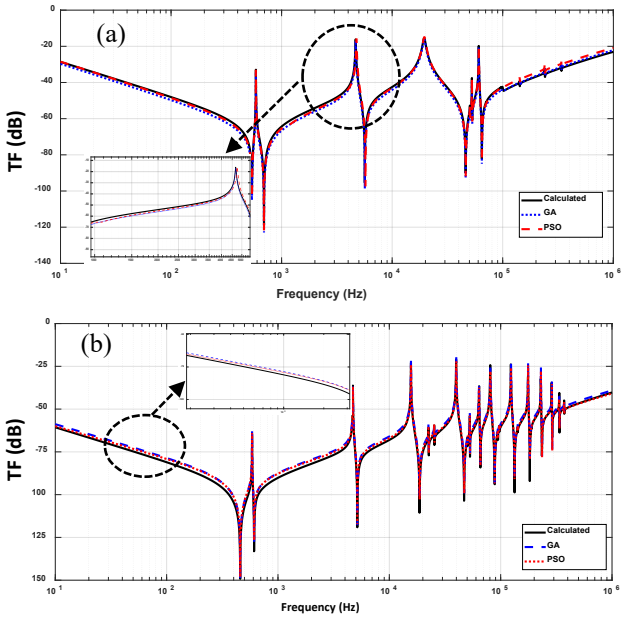

Fig. 9. Calculated and estimated FRA signatures of the 40-MVA transformer (a) LV winding and (b) HV winding.

FRA signatures of phase-A of the the LV and HV windings constructed using calculated and estimated parameters are shown in Fig. 9. Results attest the ability of the proposed techniques to estimate transformer parameters from the FRA signature. Similar to the previous case study, two levels of LV winding axial displacement are simulated through changing C_{sh} and C_{HL} by 10% and 20%. The estimated parameters for such fault and the corresponding FRA signatures are shown in Table VI and Fig. 10. The same procedure is used to estimate the parameters of the HV winding with simulated axial displacement and the results are given in Table VII and Fig. 11. Results reveal the ability of the proposed method to estimate transformer electric circuit parameters with high accuracy. Also, results in Tables III and IV reveal the reliability of the two AI techniques as both can reproduce each parameter under various transformer health conditions with acceptable consistency level.

This article has been accepted for publication in a future issue of this journal, but has not been fully edited. Content may change prior to final publication. Citation information: DOI 10.1109/TPWRD.2019.2938020, IEEE Transactions on Power Delivery

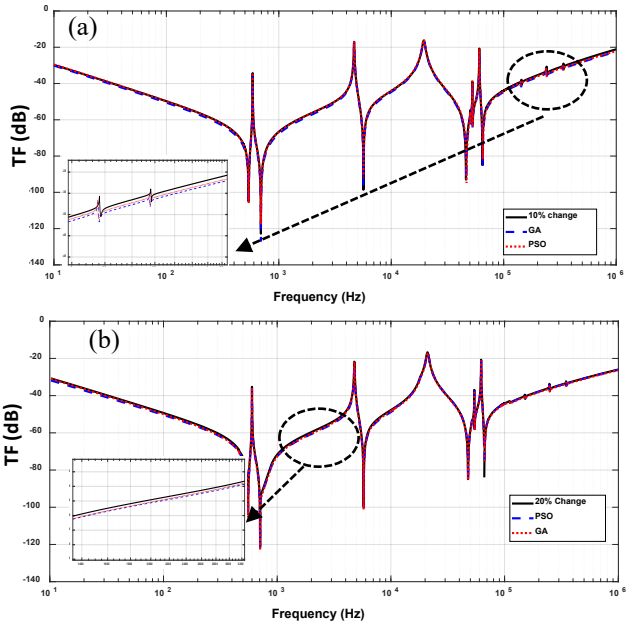

Fig. 10. Calculated and estimated FRA for the 40-MVA transformer, LV winding using GA and PSO with change in C_{sh} and C_{HL} (a)10% and (b)20%.

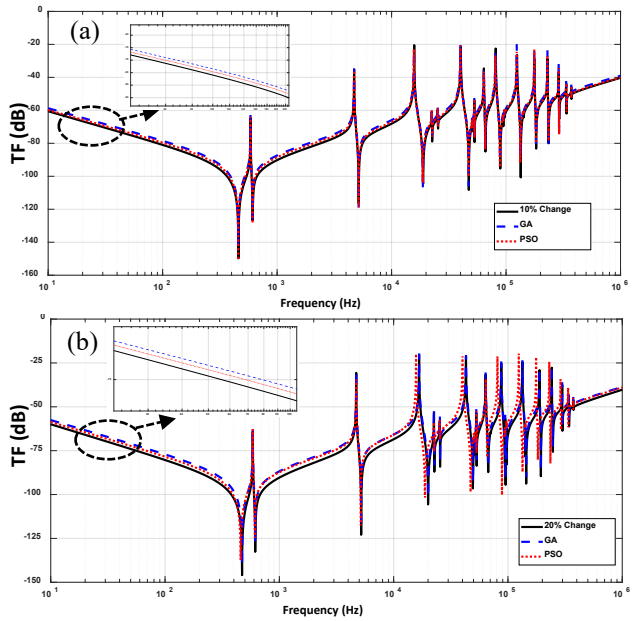

Fig. 11. Calculated and estimated FRA for the 40-MVA transformer, HV winding using GA and PSO with change in C_{sh} and C_{HL} (a)10% and (b)20%.

3. *Case study 3: Practical Implementation of the proposed technique*

The practical implementation of the proposed technique is demonstrated through its application to estimate the equivalent electric circuit parameters of a measured practical FRA signature of a 3-phase, 50 Hz, Y-Y 45 MVA, 154/23 kV, faulty transformer that was manufactured in 1989. The FRA signatures of the three phases of the LV and HV windings shown in Figs.12 and 13, respectively were measured using a commercial FRA analyser. The measured FRA signatures show a significant deviation of phase-C signature than the other two phases in the low frequency range with a change of the amplitude in the entire frequency range. This is an indication of short circuit turns [6].

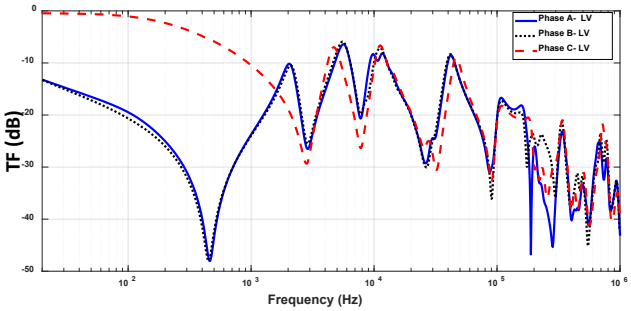

Fig.12. Measured LV-FRA of the three phases of the 45-MVA transformer.

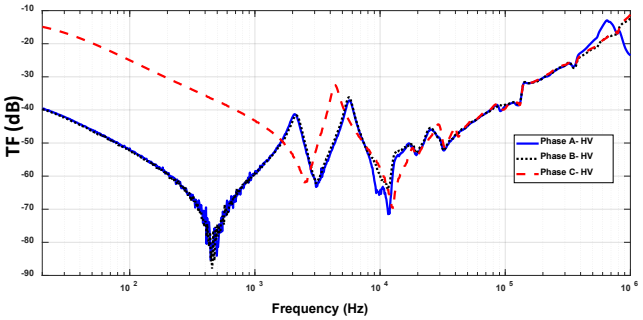

Fig.13. Measured HV-FRA of the three phases of the 45-MVA transformer.

It is to be noted that detailed physical dimensions of such old transformer are not available. So, the only way to identify the transformer equivalent circuit parameters is through estimating them from the measured FRA signature. The proposed AI techniques are employed to estimate the parameters of the individual phases of the LV and HV windings based on the measured FRA signatures shown in Figs. 12 and 13. Estimated parameters using the two AI techniques are listed in Tables VIII and IX; respectively.

Table VIII
Estimated parameters of the 45-MVA transformer LV windings

Parameters	Phase A		Phase B		Phase C	
	GA	PSO	GA	PSO	GA	PSO
R_s [Ω]	0.59	0.6	0.56	0.58	0.55	0.54
L_s [μH]	62.4	63.4	58.2	60	20.9	20.3
C_{sh} [pF]	317	318.6	319.9	329	338	332
G_{sh} [μS]	1.62	1.6	1.43	1.53	1.53	1.55
C_o [pF]	52.8	53.5	58.7	59	64	62.2
G_o [μS]	1279	1276	1270	1259	1262	1267
C_{HL} [pF]	1003	998	995	993	1053	1072
G_{HL} [μS]	528	520.6	521	534	541	529.5

Table IX
Estimated parameters of the 45-MVA transformer HV windings

Parameters	Phase A		Phase B		Phase C	
	GA	PSO	GA	PSO	GA	PSO
R_s [Ω]	1.1	0.98	0.99	0.96	0.91	0.89
L_s [μH]	113	110	117	113	55	53
C_{sh} [pF]	558	560	559	565	576	573
G_{sh} [μS]	2.41	2.5	2.1	2.34	2.46	2.4
C_o [pF]	32	33.4	33	30.2	37	35
G_o [μS]	862	875.6	876	882	889.5	879
C_{HL} [pF]	1085	1113	1140	1118	1139	1130
G_{HL} [μS]	527	538.5	539	543	576	548

As the reference data are not available for this transformer, corresponding circuit parameters of the individual phases are compared. It can be seen from Table VIII that parameters of all phases are comparable except the inductance of phase-C which is significantly reduced than the other two phases. Also, the series resistance is slightly reduced. The reduction

This article has been accepted for publication in a future issue of this journal, but has not been fully edited. Content may change prior to final publication. Citation information: DOI 10.1109/TPWRD.2019.2938020, IEEE Transactions on Power Delivery

in the series impedance results in an increase in the shunt capacitance C_0. The change in the inductance agrees well with the deviation of phase-C FRA signature in the low frequency range that is mainly dominated by the transformer inductive components. The reduction of the series impedance is an indication of a short turns fault within phase-C of the LV windings. The measured FRA signature of the HV windings shown in Fig. 13 also reveal a fault in phase-C. The practical FRA signature shown in Fig. 13 is used to estimate the parameters of the individual phases of the HV windings as listed in Table IX. Same observation on the reduction of the series impedance can be reported for phase-C of the HV windings. The fault was confirmed by unwrapping phase-C winding as shown in Fig. 14.

Fig. 14 Flashover on phase-C of the 45-MVA transformer due to the short circuit turns.

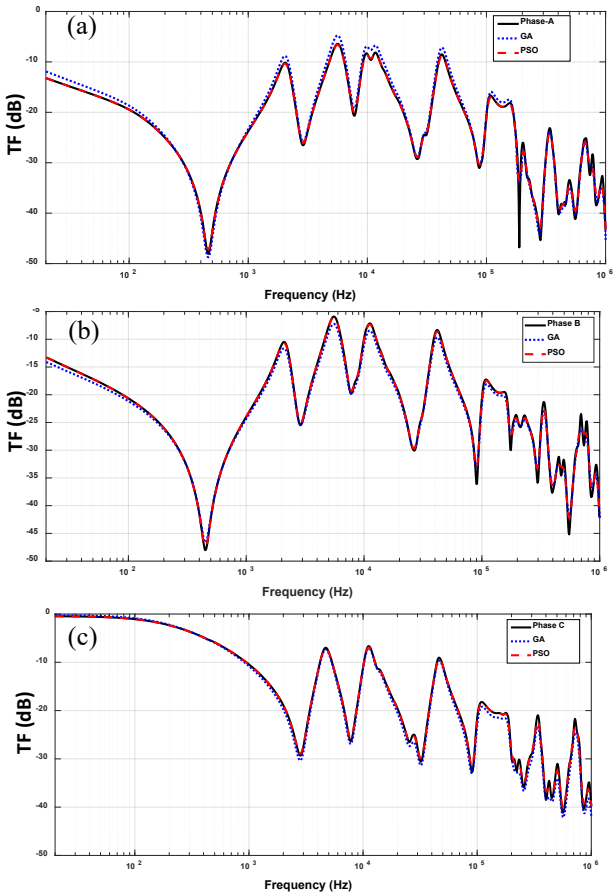

Fig. 15 Measured and estimated FRA signatures of the 45-MVA transformer LV windings (a) phase-A, (b) phase-B, (c) phase-C

The measured FRA signature of each phase is compared with the corresponding FRA signature plotted using the estimated parameters in Tables VIII and IX as shown in Figs. 15 and 16; respectively. As can be seen in these figures, measured and estimated FRA signatures are of good agreement.

With further investigations, quantitative analysis can be conducted based on the percentage change of the affected circuit parameter. In this way, automated and reliable interpretation codes for transformer FRA signatures can be established [35].

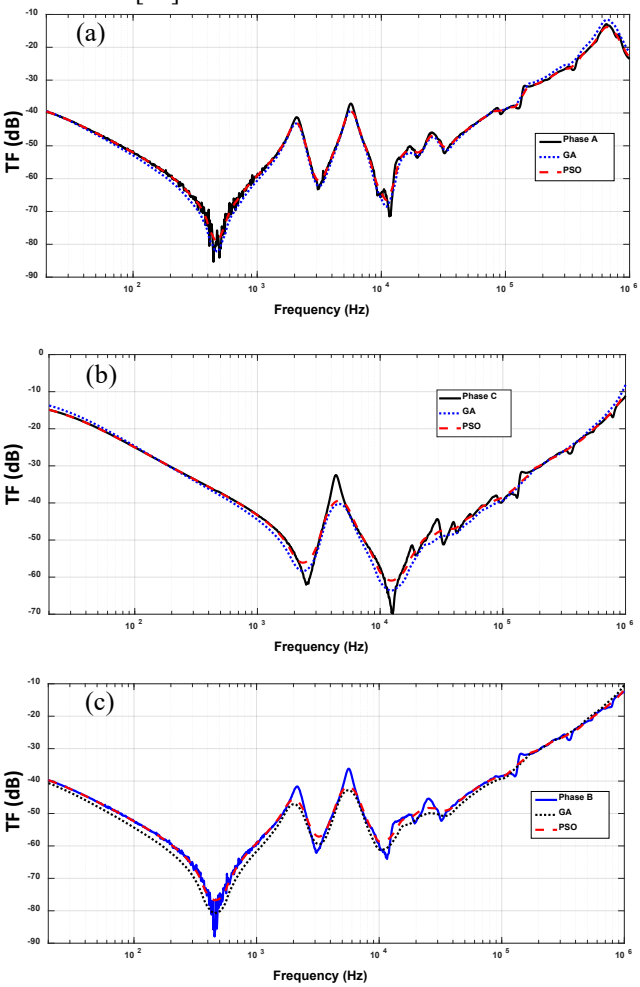

Fig. 16. Measured and estimated FRA signatures of the 45-MVA transformer HV windings (a) phase-A, (b) phase-B, (c) phase-C.

V. CONCLUSION

Current industry practice relies on graphical analysis to interpret power transformer FRA signatures. This may lead to false interpretation as so far; this process depends on personnel expertise more than standard interpretation codes. Thus, establishing reliable FRA interpretation technique based on standard numerical analysis is essential. The key conclusions of the paper and recommended future work are summarised below:

- the proposed technique can effectively estimate the parameters of the transformer high frequency electrical model from the transformer FRA signature with high accuracy.

This article has been accepted for publication in a future issue of this journal, but has not been fully edited. Content may change prior to final publication. Citation information: DOI 10.1109/TPWRD.2019.2938020, IEEE Transactions on Power Delivery

- significant deviation of a particular parameter from reference data set or from the corresponding parameter of other phases is an indication of a fault.
- fault type can be identified based on the physical meaning of the varied model parameter. fault level can be quantified based on the amount of the change in the parameter from a reference data set.
- further investigation is required to accurately correlate the percentage change in each parameter with the corresponding fault level.
- The robustness of the proposed technique should undergo further investigations on several real transformers of different ratings and operating conditions.
- The proposed estimation technique can facilitate the development of standard and automated codes for the identification and quantification of the power transformers FRA signatures.
- The proposed technique is easy to implement within commercial frequency response analysers.

VI. APPENDIX

TABLE A-I
Equations used by FEA to calculate transformer circuit parameters

Circuit parameter	Formula	Definition
Capacitance (C)	$C = \frac{\int_\Omega D_i E_j d\Omega}{v^2}$	Capacitance between two conductors i (of electric flux density D_i) and j (with electric field intensity E_j) that have a potential difference v.
Inductance (L)	$L = \frac{\int_m B \times H d\Omega}{I_p^2}$	B is the magnetic field density, H is the magnetic field intensity and Ω is the volume of the conductor
Resistance (R)	$R = \frac{\frac{1}{2\sigma}\int_m \vec{J}.\vec{J} d\Omega}{I_{rms}^2}$	σ is the conductor conductivity, J is the current density and I_{rms} is the root mean square current.

TABLE A-II
Equivalent circuit parameters for the 2-transformers simulated using FEA

Transformer parameters	10 kVA		40 MVA	
	HV	LV	HV	LV
L_s [μH], R_s [Ω]	40, 1	20, 0.5	10, 1	10.5, 0.25
C_{sh} [pF]	2.35	37.27	393.4	127.67
G_{sh} [μS]	6.45	260.89	196.7	63.835
C_o [pF]	20	718	61.192	115.53
G_o [μS]	140	5026	30.596	57.765
C_{HL} [pF], G_{HL} [μS]	50, 350		89.283, 44.65	

State space representation of transformer electric circuit model

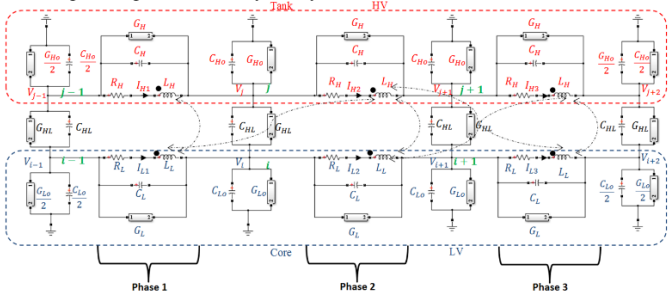

Fig. A-1. 3-Phase, Two winding transformer model

$$v_j - v_{j+1} = R_H I_j + L_H \dot{I}_j + M_{i,j}\dot{I}_i + M_{j,j-1}\dot{I}_{j-1} + M_{j,j+1}\dot{I}_{j+1} + M_{j,i-1}\dot{I}_{i-1} + M_{j,i+1}\dot{I}_{i+1} \quad (A.1)$$

$$-I_{j-1} + I_j + G_H(v_j - v_{j+1}) + C_H(\dot{v}_j - \dot{v}_{j+1}) + G_{Ho}v_j + C_{Ho}\dot{v}_j + G_{HL}(v_j - v_i) + C_{HL}(\dot{v}_j - \dot{v}_i) - I_{j-1} + G_H(v_j - v_{j-1}) + C_H(\dot{v}_j - \dot{v}_{j-1}) = 0 \quad (A.2)$$

REFERENCES

[1] A. Abu-Siada and S. Islam, "A new approach to identify power transformer criticality and asset management decision based on dissolved gas-in-oil analysis," *Dielectrics and Electrical Insulation, IEEE Transactions on,* vol. 19, pp. 1007-1012, 2012.

[2] O. Aljohani and A. Abu-Siada, "Application of Digital Image Processing to Detect Short-Circuit Turns in Power Transformers Using Frequency Response Analysis," IEEE Transactions on Industrial Informatics, vol. 12, pp. 2062-2073, 2016.

[3] M. Wang, A. J. Vandermaar, and K. D. Srivastava, "Review of condition assessment of power transformers in service," IEEE Electrical Insulation Magazine, vol. 18, no. 6, pp. 12–25, Nov./Dec. 2002.

[4] M. Bagheri, M. Lu, M. S. Naderi and B. T. Phung, "Transformer frequency response: a new technique to analyze and distinguish the low-frequency band in the frequency response analysis spectrum," in IEEE Electrical Insulation Magazine, vol. 34, no. 5, pp. 39-49, September-October 2018.

[5] M. Meira, C. R. Ruschetti, R. E. Álvarez and C. J. Verucchi, "Power transformers monitoring based on electrical measurements: state of the art," in *IET Generation, Transmission & Distribution*, vol. 12, no. 12, pp. 2805-2815, 10 7 2018.

[6] A. Abu-Siada, N. Hashemnia, S. Islam, and M. A. S. Masoum, "Understanding power transformer frequency response analysis signatures," Electrical Insulation Magazine, IEEE, vol. 29, pp. 48-56, 2013.

[7] N. Hashemnia, A. Abu-Siada, and S. Islam, "Detection of power transformer bushing faults and oil degradation using frequency response analysis," IEEE Transactions on Dielectrics and Electrical Insulation, vol. 23, pp. 222-229, 2016.

[8] K. G. N. B. Abeywickrama, Y. V. Serdyuk and S. M. Gubanski, "Exploring possibilities for characterization of power transformer insulation by frequency response analysis (FRA)," in IEEE Transactions on Power Delivery, vol. 21, no. 3, pp. 1375-1382, July 2006.

[9] O. Aljohani and A. Abu-Siada, "Application of DIP to Detect Power Transformers Axial Displacement and Disk Space Variation Using FRA Polar Plot Signature," in IEEE Transactions on Industrial Informatics, vol. 13, no. 4, pp. 1794-1805, Aug. 2017.

[10] O. Aljohani and A. Abu-Siada, "Application of digital image processing to detect transformer bushing faults and oil degradation using FRA polar plot signature," in IEEE Transactions on Dielectrics and Electrical Insulation, vol. 24, no. 1, pp. 428-436, Feb. 2017.

[11] A. Abu-Siada, O. Aljohani, "Detecting Incipient Radial Deformations of Power Transformer Windings using Polar plot and Digital Image Processing", IET Science, Measurement & Technology, Vol. 12, Issue 4, pp. 492 – 499, 2018.

[12] S. K. Mukerji, G. K. Singh, S. K. Goel, and K. P. Basu, "Measurement of Equivalent-Circuit Parameters for Single-Phase Transformers with Unknown Turns-Ratio and Large Series-Branch Impedances," in 2006 International Conference on Electrical and Computer Engineering, 2006, pp. 353-356.

[13] S. Chapman, Electric machinery fundamentals: Tata McGraw-Hill Education, 2005.

[14] S.-D. Cho, "Three-phase transformer model and parameter estimation for ATP," Journal of Electrical Engineering and Technology, vol. 1, pp. 302-307, 2006.

[15] M. I. Mossad, M. Azab, and A. Abu-Siada, "Transformer Parameters Estimation From Nameplate Data Using Evolutionary Programming Techniques," IEEE Transactions on Power Delivery, vol. 29, pp. 2118-2123, 2014.

[16] Q. Wu, S. Jazebi, and F. d. Leon, "Parameter Estimation of Three-Phase Transformer Models for Low-Frequency Transient Studies from Terminal Measurements," IEEE Transactions on Magnetics, vol. PP, pp. 1-1, 2016.

[17] R. Mohamed, I. Markovsky, and P. L. Lewin, "Modeling and Parameter Estimation of High Voltage Transformer Using Rational Transfer

Function State Space Approach," in 2008 Annual Report Conference on Electrical Insulation and Dielectric Phenomena, 2008, pp. 467-470.
[18] D. Aguglia, P. Viarouge, and C. d. A. Martins, "Frequency-Domain Maximum-Likelihood Estimation of High-Voltage Pulse Transformer Model Parameters," IEEE Transactions on Industry Applications, vol. 49, pp. 2552-2561, 2013.
[19] E. S. Jin, L. L. Liu, Z. Q. Bo, and A. Klimek, "Parameter identification of the transformer winding based on least-squares method," in 2008 IEEE Power and Energy Society General Meeting - Conversion and Delivery of Electrical Energy in the 21st Century, 2008, pp. 1-6.
[20] S. Jazebi, A. Rezaei-Zare, M. Lambert, S. E. Zirka, N. Chiesa, Y. I. Moroz, et al., "Duality-Derived Transformer Models for Low-Frequency Electromagnetic Transients- Part II: Complementary Modeling Guidelines," IEEE Transactions on Power Delivery, vol. 31, pp. 2420-2430, 2016.
[21] V. Rashtchi, E. Rahimpour, and H. Fotoohabadi, "Parameter identification of transformer detailed model based on chaos optimisation algorithm," IET Electric Power Applications, vol. 5, pp. 238-246, 2011.
[22] L. Satish and A. Saravanakumar, "Identification of Terminal Connection and System Function for Sensitive Frequency Response Measurement on Transformers," in IEEE Transactions on Power Delivery, vol. 23, no. 2, pp. 742-750, April 2008.
[23] M. Steurer, W. Hribernik and J. H. Brunke, "Calculating the transient recovery voltage associated with clearing transformer determined faults by means of frequency response analysis," in IEEE Transactions on Power Delivery, vol. 19, no. 1, pp. 168-173, Jan. 2004.
[24] Shintemirov, W. H. Tang and Q. H. Wu, "Transformer Core Parameter Identification Using Frequency Response Analysis," in IEEE Transactions on Magnetics, vol. 46, no. 1, pp. 141-149, Jan. 2010.
[25] A. Keyhani, S. W. Chua and S. A. Sebo, "Maximum likelihood estimation of transformer high frequency parameters from test data," in IEEE Transactions on Power Delivery, vol. 6, no. 2, pp. 858-865, April 1991.
[26] B. Gustavsea and A. Semlyen, "Rational approximation of frequency domain responses by vector fitting," IEEE Trans. Power Del., vol. 14, no. 3, pp. 1052–1061, Jul. 1999.
[27] B. Gustavsen and C. Heitz, "Modal Vector Fitting: A Tool For Generating Rational Models of High Accuracy With Arbitrary Terminal Conditions," in IEEE Transactions on Advanced Packaging, vol. 31, no. 4, pp. 664-672, Nov. 2008.
[28] X. Zhao, Chenguo Yao, A. Abu-Siada, Ruijin Liao, "High Frequency Electric Circuit Modeling for Transformer Frequency Response Analysis Studies", International Journal of Electrical Power and Energy Systems, Vol. 111, pp. 351-368, April 2019.
[29] S. J. Russell, P. Norvig, J. F. Canny, J. M. Malik, and D. D. Edwards, Artificial intelligence: a modern approach vol. 2: Prentice hall Upper Saddle River, 2003.
[30] M. I. Mosaad , M Azab and A.Abu Siada "A Novel Evolutionary Technique to Estimate Induction Machine Parameters from Name Plate Data"ICEM'2016 SwissTech Convention Center Lausanne–Switzerland, September 4-7, 2016.
[31] M. Azab, Fawzan Salem and M. I. Mosaad "PV parameters estimation using EC Techniques" Journal of Electrical Engineering JEE, Volume 13/2013 - Edition: 4, 187 - 195.
[32] D. E. Golberg, "Genetic algorithms in search, optimization, and machine learning," Addion wesley, vol. 1989, p. 102, 1989.
[33] Y. d. Valle, G. K. Venayagamoorthy, S. Mohagheghi, J. C. Hernandez, and R. G. Harley, "Particle Swarm Optimization: Basic Concepts, Variants and Applications in Power Systems," IEEE Transactions on Evolutionary Computation, vol. 12, pp. 171-195, 2008.
[34] N. Hashemnia, A. Abu-Siada, and S. Islam, "Improved power transformer winding fault detection using FRA diagnostics part 1: axial displacement simulation," Dielectrics and Electrical Insulation, IEEE Transactions on, vol. 22, pp. 556-563, 2015.
[35] Naser Hashemnia, A. Abu-Siada, Mohammad A.S. Masoum, and Syed M. Islam, "Characterization of Transformer FRA Signature under Various Winding Faults", proceeding of the Condition Monitoring and Diagnosis conference, Bali, Indonesia, September 2012.

A. Abu-Siada (M'07, SM'12) received the B.Sc. and M.Sc. degrees from Ain Shams University, Egypt in 1998 and the PhD degree from Curtin University, Australia in 2004, all in Electrical Engineering. Currently he is an associate professor and lead of the Electrical and Electronic Engineering discipline at Curtin University. His research interests include power system stability, condition monitoring, power electronics and power quality. He has published over 230-research paper, book and book chapters in these research areas. He is Editor-in-Chief of the international journal Electrical and Electronic Engineering, regular reviewer for various IEEE Transactions and vice-chair of the IEEE Computation Intelligence Society, WA Chapter.

Mohamed I. Mossad received his PhD degree from Cairo University, Egypt, in electrical engineering. Currently he is an assistant professor in the Department of Electrical and Computer Engineering at the Higher Technological Institute, Egypt, on leave to Yanbu Industrial College, Saudi Arabia. His research interests include power system stability, control and renewable energy. He is a regular reviewer for the International Journal of Industrial Electronics and Drives and International Journal of Energy Engineering.

Dowon Kim received the B.Sc. and M.Sc. degrees in electrical engineering from the Seoul National University of Science and Technology, Seoul, South Korea, in 2003 and 2009, respectively. He is currently pursuing the Ph.D. degree with Curtin University, Australia. From 1998 to 2011, he was a Transmission and Substation Engineer and an Engineering Lecturer with Korea Electric Power Corporation, Seoul. He was a Senior Testing and Commissioning Engineer with Global Testing Services, Australia until 2016. His current research interests include wireless power transfer systems, frequency response, high-voltage condition monitoring, and power system protection.

M. F. El-Naggar received the B.Sc., M.Sc. and Ph.D. degrees, all in electrical engineering, from Helwan University, Egypt in 1995, 2002 and 2009; respectively. He has been working as an associate professor at the Power and Electrical Machines Department, Faculty of Engineering, Helwan University, Egypt. Currently, he is an assistant professor at the Department of Electrical Engineering, Sattam Bin Abdul Aziz University, Saudi Arabia. His main research interests include power system protection, power transformers operation, smart grids, renewable energy, and image processing.